UT simulation using a fully automated 3D hybrid model: Application to planar backwall breaking defects inspection

Alexandre Imperiale, Sylvain Chatillon, Michel Darmon, Nicolas Leymarie, Edouard Demaldent

UT Simulation Using a Fully Automated 3D Hybrid Model: Application to Planar Backwall Breaking Defects Inspection

Alexandre Imperiale, Sylvain Chatillon, Michel Darmon,
Nicolas Leymarie and Edouard Demaldent

CEA, LIST, 91191Gif-sur-Yvette, France

Corresponding author: alexandre.imperiale@cea.fr

Abstract. The high frequency models gathered in the CIVA software allow fast computations and provide satisfactory quantitative predictions in a wide range of situations. However, the domain of validity of these models is limited since they do not accurately predict the ultrasound response in configurations involving subwavelength complex phenomena. In addition, when modelling backwall breaking defects inspection, an important challenge remains to capture the propagation of the creeping waves that are generated at the critical angle. Hybrid models combining numerical and asymptotic methods have already been shown to be an effective strategy to overcome these limitations in 2D [1]. However, 3D simulations remain a crucial issue for industrial applications because of the computational cost of the numerical solver. A dedicated three dimensional high order finite element model combined with a domain decomposition method has been recently proposed to tackle 3D limitations [2]. In this communication, we will focus on the specific case of planar backwall breaking defects, with an adapted coupling strategy in order to efficiently model the propagation of creeping waves. Numerical and experimental validations will be proposed on various configurations.

INTRODUCTION

UT simulation codes embedded into the CIVA software platform [1] allow predicting beam propagation as well as flaw response in echographic mode for various techniques (pulse echo, TOFD, Tandem) and probes (monolithic, dual RT or phased arrays [3]) in arbitrary components (homogeneous/heterogeneous, isotropic/anisotropic, canonical or CAD geometry). The high frequency approximation models – such as ray-based models – gathered in CIVA allow fast computations, a crucial requirement in the industrial context, and provide quantitative predictions but with a well-known limited range of validity. Ray models fail at predicting responses from defects in some complex configurations, e.g., critical phenomena, such as head waves generated at the critical angle, creeping waves or caustics. In the same way, their precision drops for defects with characteristic dimension of the order of the wavelength. Finally, when defects of complex geometry or neighboring defects are considered, the complete scattering processes are not taken into account. To overcome these limitations, a hybrid approach combining ray based and numerical models has been implemented in CIVA, and in the following we illustrate and validate this approach in the case of surface breaking flaws.

HYBRID APPROACH USING RAY-BASED AND NUMERICAL MODELS

The approach promoted in CIVA is to use as much as possible fast asymptotic solutions within their range of validity. In practice, this range of validity is usually limited to propagation in healthy environment (specimen without flaw) or to certain types of defects, of relatively simple geometry.

Numerical schemes such as FEM do not rely on asymptotic approximations for computations of elastic waves phenomena, thus ensuring the accuracy of the model. However, the computational cost (computation time and memory load) of numerical schemes are potentially prohibitive for three dimensional problems, when considering the typical wave paths of hundreds of wavelengths in NDT configurations. Thereby, 3D simulations remain a crucial issue for industrial applications, hence enhancing the interest for numerical/asymptotic hybrid approaches.

The main principle of such coupling is to use the computation of the incident field from CIVA applying the beam computation module [3], and to compute the interaction with the flaw using a dedicated numerical model. The echo-response from the defect is then given by the Auld's reciprocity principle [4], which links healthy (incident field) and flawed (defect's scattering) components.

44th Annual Review of Progress in Quantitative Nondestructive Evaluation, Volume 37
AIP Conf. Proc. 1949, 050004-1–050004-8; https://doi.org/10.1063/1.5031546
Published by AIP Publishing. 978-0-7354-1644-4/$30.00

The input data of the numerical model is obtained in an area of interest associated with the defect using a ray based beam computation model in the healthy part. The contributions of the defect subject to this incident field are then computed using the numerical model. The elastodynamic response is then obtained by applying the Auld principle of reciprocity [4]. In harmonic regime, for a spectrum of the input signal S_i, the elastodynamic response spectrum S_e of a defect with a surface Σ is expressed as

$$S_e = S_i \int_{\Sigma} \left(\mathbf{u}_E \cdot \mathbf{T}_R - \mathbf{u}_R \cdot \mathbf{T}_E \right) d\Sigma,$$

where u and T denote the displacement vector and the normal stress tensor of the harmonic fields. The indexes E and R denote the two following states of the configuration: E is the ultrasonic field radiated by the emitting probe in the healthy component; R is the ultrasonic field radiated by the reception sensor (used as a fictitious emitter) in the presence of the defect. The reciprocity signal previously expressed is the starting point of our hybrid strategy, since it enables the separation between the computation of the incident field and the diffracted field.

The coupling strategy has already been applied to a hybrid code combining the CIVA beam computation module with the FEM code ATHENA, developed by EDF, investigated and validated for 2D configurations [5]. For example, the capabilities of this hybrid method have been highlighted when simulating the inspection of various surface breaking notches. The specificity of this numerical model lies in the contribution of the flaw geometry, handled by the fictitious domain method. This strategy is particularly efficient in 2D cases, but in practice becomes hardly scalable for 3D cases.

To gain in performances in order to meet the needs of industrial applications to deal with more complex configurations, we propose a variant of the coupling. This variant is based, first, on a parametric representation of the defect together with a dedicated domain decomposition method and, second, on using the high order spectral finite element method.

DESCRIPTION OF THE NUMERICAL MODEL

More specifically, we coined the term “dedicated” 3D hybrid model since, rather than constituting a generic FEM solver based upon any geometrical mesh of the defect (or of its surrounding), we aim at building a lexicon of parametric defects – that corresponds to those mostly encountered in NDT configurations. This lexicon is internally queried by the CIVA software, in a transparent way for the end user. Each parametric defect is associated with a composition of geometrical structures referred to as macro-elements. In essence, a macro-element is defined as a potentially nonlinear deformation of a reference cube, and the complete set of macro-elements are arranged altogether in order to fit the defect geometrical description. The reference cube also bears a predefined hexahedral mesh, so that a macro-element inherits from this mesh through its associated deformation. As an illustration of how the constitution of macro-elements is performed, Fig. 1 proposes such decomposition in a simpler 2D case where a parametrized 2D edge representing a crack is given as an input. It should be noted that in Fig. 1, the absorbing layers used to model an infinite domain around the flaw are intentionally omitted to simplify the presentation, whereas in practice Perfectly Matched Layers (PMLs) [9] are used. The communications between each macro-element are enabled using the mortar element method [8] as a mean of domain decomposition.

Computational performances, within each subdomain, are significantly enhanced by the use of high order spectral finite elements [6, 7] defined on hexahedral meshes. This numerical method is widely spread in the community of numerical solutions of transient high-frequency wave propagation problems since they combine the flexibility of finite element methods and the performances of standard finite differences by allowing a fully explicit numerical scheme thanks to a diagonal mass matrix. In the literature, this technique is referred to as the mass-lumping technique. Moreover, by allowing high order polynomials to represent the solutions, spectral finite elements require less discretization points to reach a given precision, which is a major asset when simulating 3D configurations.

Moreover, the performances of the numerical solver can be increased by taking into account the parametrization of the subdomain, inherited from the parametrization of the defect. Indeed, incorporating in our formulation the fact that each macro-element is a deformed cube, we can internally define optimal data structures for performing parallelized computations along with “on-the-fly” finite element operations. Typically, the so-called stiffness matrix is never to be assembled, but is only represented as a set of local – i.e., per mesh element – matrices and the manipulation of these local matrices are performed in parallel, thus significantly decreasing CPU time and memory loads. [2].

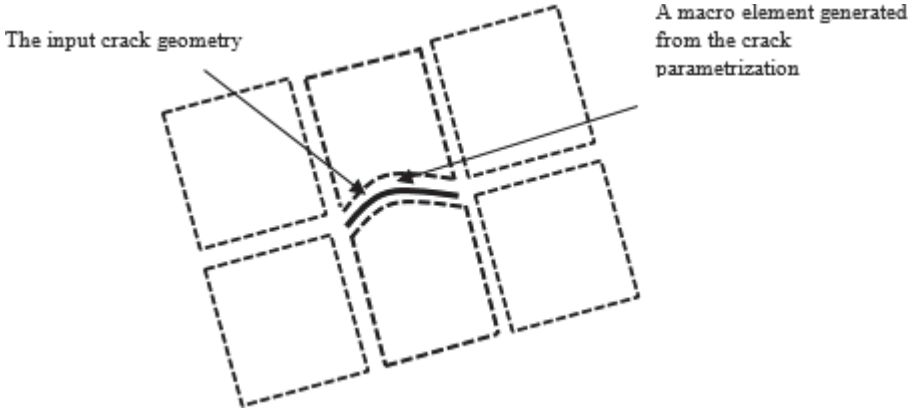

FIGURE 1. Illustration of the macro elements arranged around an embedded crack.

To assess the simulation improvement of the proposed 3D hybrid method, it will be compared to experimental results and to existing CIVA models: the asymptotic PTD model [10] (based on PTD [11]) and another coupling method (2D CIVA/ATHENA [5]).

NUMERICAL AND EXPERIMENTAL VALIDATIONS ON EMBEDDED FLAWS

For introducing this new coupling approach in CIVA software, we consider at first the response from embedded defects. This first step has been implemented in the development release of CIVA for the case of a 3D planar crack embedded in a homogeneous isotropic material. The numerical domain follows the macro-element strategy detailed in the previous section and is illustrated in Fig. 2.

As a first simulation example, we have considered a 200 x 50 x 75 mm3 of steel material, a 5 MHz transducer with 70% bandwidth and a planar square defect of 1 mm length, embedded at a 25 mm depth. The FE diffracted field obtained from the local elastic field, numerically computed, is presented in Fig. 2. It should be emphasized that the numerical solution is obtained without any intervention of the end-user, every numerical parameter being automatically deduced from the parameters of the configuration.

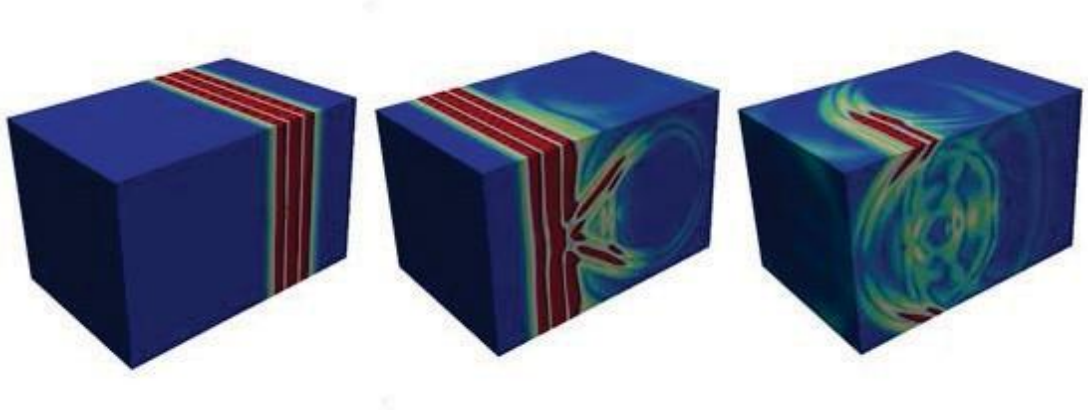

FIGURE 2. Snapshots of the transient numerical solution internally computed by CIVA to obtain the total acoustic field in a surrounding of the crack.

Experiments have been performed on small flaws compared to the wavelength. To study small ratios of flaw size/wavelength, low frequency transducers (0.5 MHz and 1 MHz) in immersion mode have been used to inspect 5mm high electro eroded slots. The following specimen (Fig. 3) has been inspected in different classical NDT configurations.

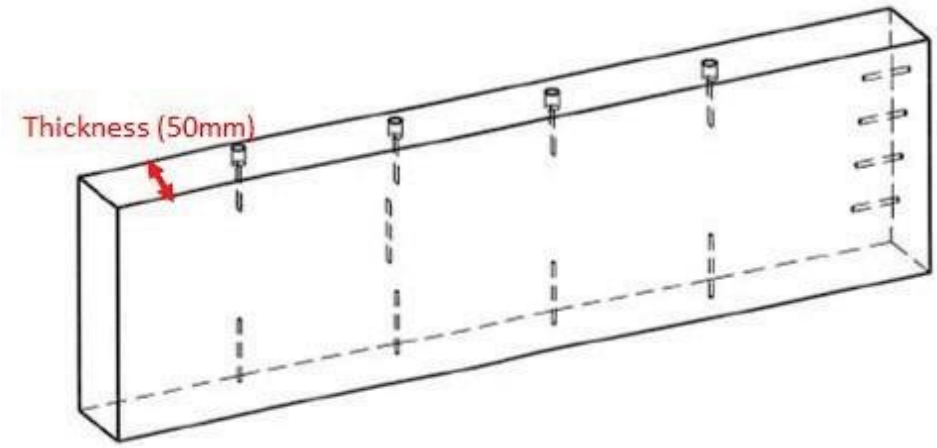

FIGURE 3. Specimen used for the following experimental validations.

The experimental validations presented here concern the 5mm height and 30mm extension notch of ligament 20mm for which the experiments are the most reliable because it is the defect farthest from specimen surfaces. Corroborating checks have however been made on other exploitable flaws. The specimen being 50mm thick the center of the defect (height 5 * extension 30mm) used in validation and of 20mm bottom ligament is thus located at a depth of 27.5mm. A 10mm extent starter hole was pre-dilled to then design the notch of 30mm extension by electro erosion.

In the studied configurations, the incident plane of the probes is perpendicular to the notch extension which is very large; consequently the flaw height can be used in good approximation to evaluate the flaw size/wavelength ratio.

The reproducibility of the results has been checked; the confidence interval of the experimental data presented in this paper has been evaluated to *+/- 3dB*. Side-drilled holes have been used for amplitude calibration and for determination of the input signal in simulation [12].

To highlight the improvement of the simulations provided by the hybrid model, measurements using shear waves have been performed with a great interest in pulse echo configurations since previous numerical validations have shown that differences between the numerical and analytical models are more important in this case [10]. Figure 4 describes the two pulse echo immersion inspections carried out at 0.5 and 1 MHz of the embedded planar electro eroded slots (shown in Fig. 3) using S45° immersion probes. As an example the experimental BScan obtained when scanning the four notches and the flat bottom holes at 0.5 MHz is given in Figure 4.b. This experimental True Bscan (representation of the maximal echo amplitude versus the scanning position and the depth with superimposition of the specimen geometry) chronologically displays the emission echo, the entry surface entry echo, the echoes generated by the flaws. The response of the specimen right corners and of the flat bottom holes is surrounded in yellow while that of the less deep notch (used for the validation here) obtained in direct mode is indicated by the blue arrow. The ultrasonic response of an embedded notch is chronologically composed of the direct, corner and indirect echoes. For the two deepest notches (at left), these echoes are rather superimposed and we well observe when comparing the responses of the four notches that the corner echo amplitude increases with decreasing THE notch backwall ligament.

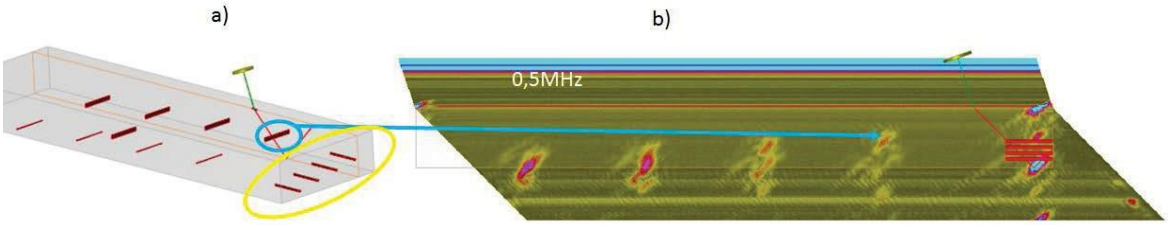

FIGURE 4. a) Pulse Echo S45° immersion inspection of several embedded planar electro eroded slots, b) experimental True BScan obtained when scanning the notches and the flat bottom holes at 0.5 MHz. The specimen is represented by gray lines and the flaws are in red.

The table in Fig. 5a shows that the hybrid model provides simulated results close to the experimental ones (disagreement less than 3 dB) whereas the PTD model is less effective. Note that an 8,1dB difference between PTD

and FEM is obtained at 0,5Mhz; this confirms that PTD well deviates from a numerical simulation for small flaw size/wavelengths ratios. The echo waveform is also rather well modeled by the hybrid model (see Ascans with or without normalization in Fig. 5b and c.

a)

Gap Simulation/Exp (dB)	0,5MHz	1MHz
3D FEM	+2,5	0,0
PTD 3D	-5,6	-4,0

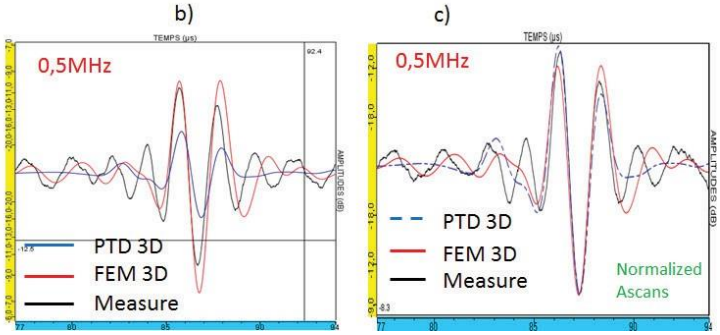

FIGURE 5. Gap simulation/experience for the 3D hybrid FEM model and for the 3D PTD model
b) Superimposition of the experimental AScan and simulated ones at 0.5 MHz, c) normalized Ascans.

The previous validation confirms that the FEM-based 3D hybrid model could bring an interesting contribution to the simulation of small defects compared to the wavelength for shear waves.

NUMERICAL AND EXPERIMENTAL VALIDATIONS ON BACKWALL BREAKING FLAWS

Experiments have been performed on backwall breaking flaws in configurations for which the asymptotic semi-analytical models as PTD are supposed to provide a less effective prediction: such configurations involve, for instance, small flaws compared to the wavelength, head waves and 3D effects (e.g., finite extension, nonzero aperture, disorientation of the flaw).

In the framework of the first validation, SV45° corner echoes of backwall breaking notches of different heights varying from 0.5 mm to 15 mm have been measured using a pulse echo inspection with an immersion Ø6.35mm probe emitting SV45° refracted waves at 2.25MHz (Fig. 6). Parameters under investigation in this validation are:

- The "notch height": knowing the limitation of the PTD model for small defect heights, we decided to compare the evolution of echoes amplitude versus height for PTD, for the FEM-based 3D hybrid model and for measurements. Corner echoes emanating from backwall breaking notches are mainly specular echoes but the effect of edge and secondary Rayleigh diffraction increases for decreasing height and the Rayleigh diffraction are not accounted for the moment in the CIVA PTD model.
- The "divergence of the probe": since the used probe of small diameter (Ø6.35mm) is planar, there are possibly some contributions to the corner echo due to creeping waves propagating both along the backwall (33° incidence angle with respect to the vertical axis) and along the flaw (57° incidence).

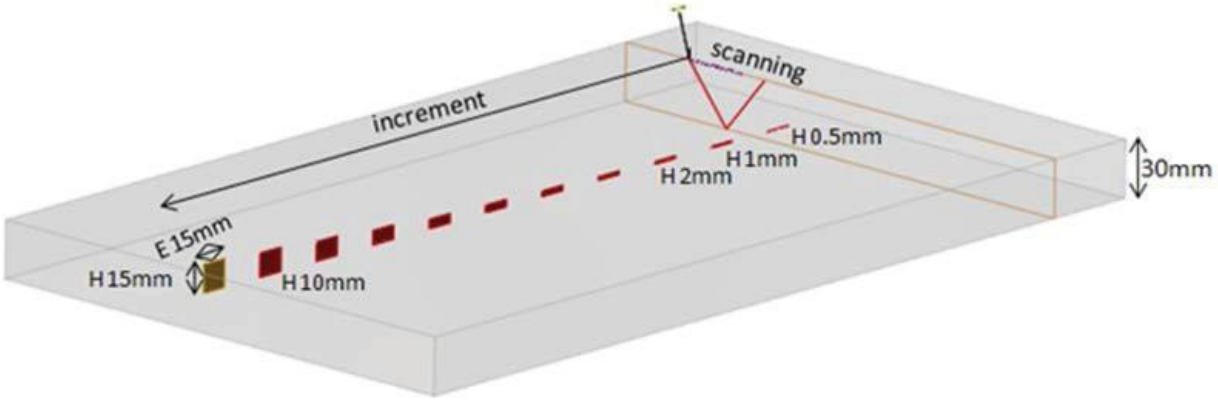

FIGURE 6. SV45° corner echoes of back-wall breaking notches of different heights.

Figure 7 compares the evolution of echoe amplitude versus height between the different models. The measure shows first that PTD breaks down in the red rectangle of Fig. 7, i.e., ka<5, ka being the dimensionless wave number, product of the wave number k by the flaw half-height a. The FEM-based 3D hybrid model (ECHO) logically over performs PTD for small flaws heights. ECHO errors are always less than measurement uncertainties (~2dB). [**HELP**

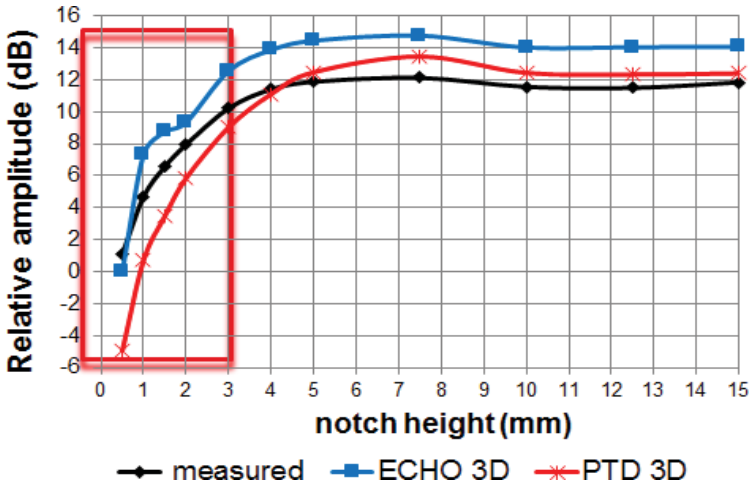

FIGURE 7. Evolution of the notches echoes amplitude versus height (varying from 0.5 mm to 15 mm) for PTD, for the FEM-based 3D hybrid model (called ECHO3D) and for measurements for the inspection depicted in Fig. 6.

The second numerical and experimental validation deals with SV45° corner echoes of backwall breaking notches of different heights, extensions and skews. This configuration involves 3D effects (finite extension, nonzero aperture, and disorientation of the flaw). Nine defects of 0.5, 1.5 and 2.5mm heights and 2, 5 and 12 mm extension (Fig. 8) have been inspected in Pulse Echo S45 contact mode using a contact monoelement 6.35mm diameter planar probe emitting SV45° waves at 2.25 MHz. A probe rotation is operated from -20° to 20° skew.

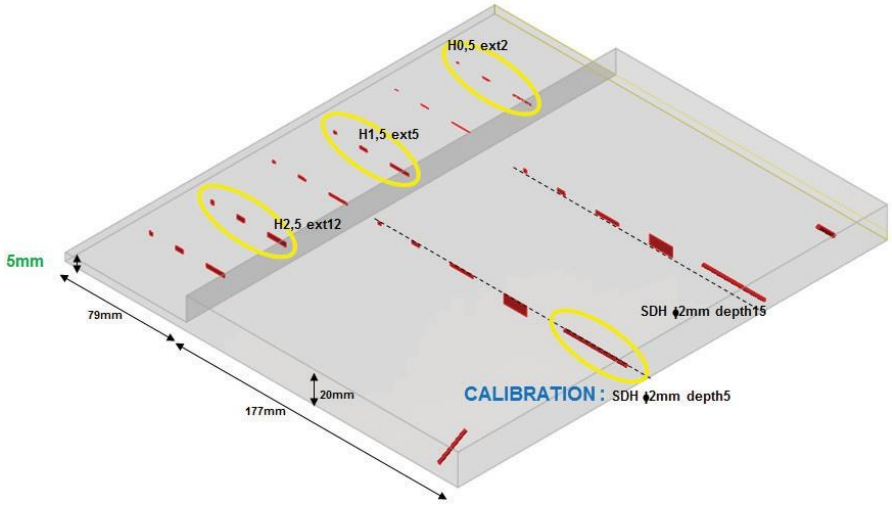

FIGURE. 8: Back-wall breaking notches of different heights (0.5, 1.5 and 2.5mm) and extensions (2, 5 and 12 mm) and the Ø2mm calibration SDH.

Figure 9 depicts the 0° skew inspection the variation of the notches echoes amplitude versus height (0.5, 1.5 and 2.5 mm) for PTD, for the FEM-based 3D hybrid model (called ECHO3D) and for measurements. The validity of the PTD prediction decreases with decreasing extension: it shows validity limitations of the PTD incremental model [10, 13] near the flaw corners. ECHO leads to a very good agreement except for the 0,5mm height (3-4dB error). For the 0,5mm height, it is needed to account for the notch opening (0,32mm) as proven by the 2D Athena simulation of a multifaceted opened flaw, such flaw shape being not available for the moment with the ECHO simulation.

Comparing the simulated echoes amplitudes for skews from -20° to 20° to measure (Fig. 10) shows a very good overall prediction provided by ECHO whereas PTD breaks down for 2mm extension due to a quantitatively imprecise prediction of the flaw corners. For 5mm extension PTD errors are probably due to the divergence of the probe and the important effect of head and Rayleigh waves for small defects, phenomena not accounted for in the CIVA PTD model.

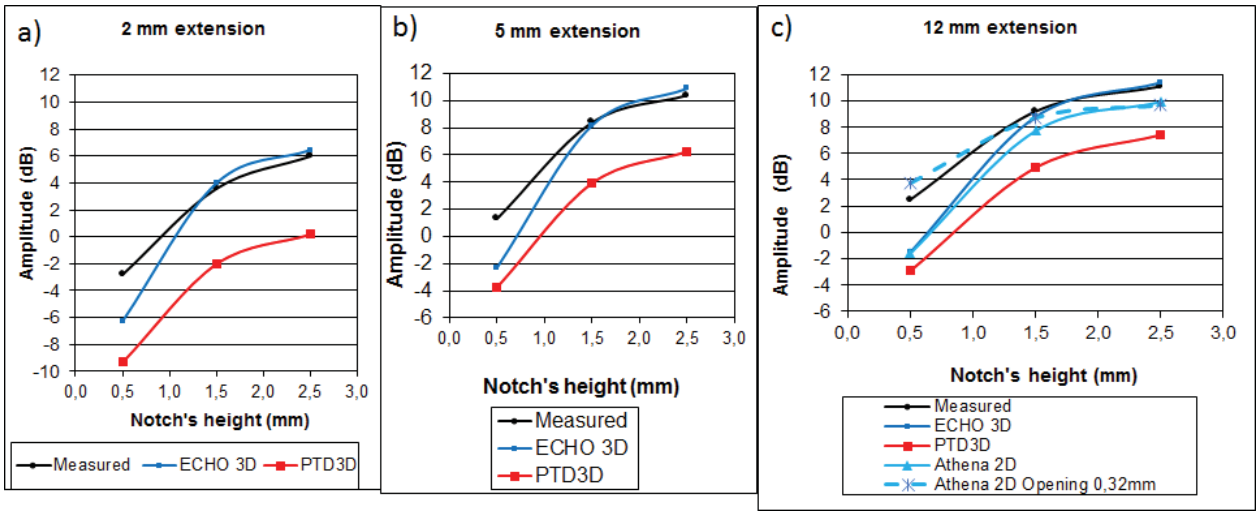

FIGURE 9. Evolution of the notch echoes amplitude versus height (0.5, 1.5 and 2.5 mm) for PTD, for the FEM-based 3D hybrid model (called ECHO3D) and for measurements for the 0° skew inspection of the specimen of Fig. 8. For 12mm extension (c), addition of the results simulated by CIVA/Athena 2D for notches of respective 0 and 0.32mm opening.

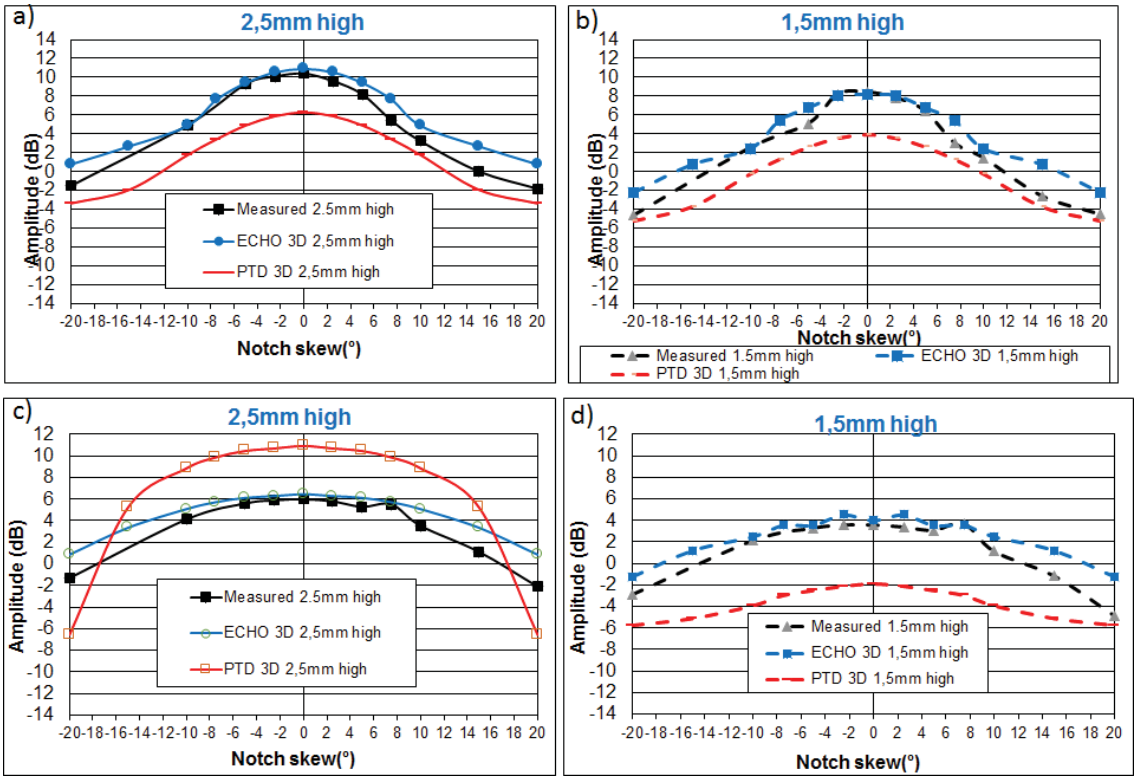

FIGURE 10. Evolution of the notch echoes amplitude versus skew (from -20° to 20°) for the notches of 5mm extension (a and b) and 2mm extension (c and d) and of 2.5 (a and c) and 1.5mm heights (b and d) for PTD, for the FEM-based 3D hybrid model (called ECHO3D) and for measurements for the inspection of the specimen depicted in Fig. 8.

CONCLUSION

An original hybrid asymptotic/numerical approach has been introduced to handle small 3D defects in the modeling of UT configurations. The numerical part is based on a high order spectral finite element method combined with a domain decomposition strategy, which is used to fit the shape of the defect. So far, this strategy has been successfully introduced in CIVA for 3D planar embedded defects and is totally transparent for the CIVA end-user. We have presented comparisons with the CIVA semi-analytical models. First numerical and experimental validations for embedded and backwall breaking planar defects have shown that the proposed 3D hybrid method leads to a significant improvement for simulating small flaws, notably for shear waves.

REFERENCES

[1] More details about CIVA, references and all the Benchmarks results can be found on the EXTENDE website http://www.extende.com.

[2] S. Mahaut, S. Chatillon, M. Darmon, N. Leymarie, R. Raillon and P. Calmon, "An Overview of Ultrasonic Beam Propagation and Flaw Scattering Models in the CIVA Software", Review of Progress in Quantitative Nondestructive Evaluation (QNDE). **29B**, pp. 2133-2140, (2009).

[3] N. Gengembre and A. Lhémery, Ultrasonics **38**:495-499, (2000).

[4] B. A. Auld, "General electromechanical reciprocity relations applied to the calculation of elastic wave scattering coefficients," *Wave motion*, **1**(1): 3-10.N. (1979).

[5] S. Mahaut, N. Leymarie, C. Poidevin, T. Fouquet, O. Dupond , "Study of complex ultrasonic NDT cases using hybrid simulation method and experimental validation," *Insight*, **53**, N°12, (Dec. 2011).

[6] G. Cohen, "Higher-order numerical methods for transient wave equations," *Springer Science & Business Media*, (2013).

[7] D. Komatitsch, J. Tromp, "Introduction to the spectral element method for three-dimensional seismic wave propagation," Geophysical journal international, **139**(3): 806-822, (1999).

[8] F. Ben Belgacem, Y. Maday, "The mortar element method for three dimensional finite elements", RAIRO-Modélisation mathématique et analyse numérique, **31**(2): 289-302, (1997).

[9] E. Demaldent, S. Imperiale, "Perfectly matched transmission problem with absorbing layers: Application to anisotropic acoustics in convex polygonal domains," *International Journal for Numerical Methods in Engineering*, **96**(11): 689-711, (2013).

[10] M. Darmon, V. Dorval, A. Kamta Djakou, L. Fradkin, and S. Chatillon, "A system model for ultrasonic NDT based on the Physical Theory of Diffraction (PTD)," *Ultrasonics*, **64**: 115–127, (Jan. 2016).

[11] V. Zernov, L. Fradkin, and M. Darmon, "A refinement of the Kirchhoff approximation to the scattered elastic fields," *Ultrasonics*, **52**(7): 830–835, (2012).

[12] M. Darmon and S. Chatillon, "Main features of a complete ultrasonic measurement model - Formal aspects of modeling of both transducers radiation and ultrasonic flaws responses," *Open J. Acoust.*, **3A**, (2013).

[13] A. Kamta Djakou, M. Darmon, and C. Potel, "Models for extending GTD to finite length defects," unpublished.